

Research Article

Experimental Research on Passive Residual Heat Removal System of Chinese Advanced PWR

Zhuo Wenbin, Huang Yanping, Xiao Zejun, Peng Chuanxin, and Lu Sansan

CNNC Key Laboratory on Nuclear Reactor Thermal Hydraulics Technology, Nuclear Power Institute of China, Chengdu 610041, China

Correspondence should be addressed to Zhuo Wenbin; npic011371@163.com

Received 6 December 2013; Accepted 24 February 2014; Published 5 June 2014

Academic Editor: Shengqiang Li

Copyright © 2014 Zhuo Wenbin et al. This is an open access article distributed under the Creative Commons Attribution License, which permits unrestricted use, distribution, and reproduction in any medium, provided the original work is properly cited.

Passive residual heat removal system (PRHRS) for the secondary loop is one of the important features for Chinese advanced pressurized water reactor (CAPWR). To prove the safety characteristics of CAPWR, series of experiments have been done on special designed PRHRS test facility in the former stage. The test facility was built up following the scaling laws to preserve the similarity to CAPWR. A total of more than 300 tests have been performed on the test facility, including 90% steady state cases and 10% transient cases. A semiempirical model was generated for passive heat removal functions based on the experimental results of steady state cases. The dynamic capability characteristics and reliability of passive safety system for CAPWR were evidently proved by transient cases. A new simulation code, MISAP2.0, has been developed and calibrated by experimental results. It will be applied in future design evaluation and optimization works.

1. Introduction

The passive safety feature is one important essential requirement for both integral type reactors and large scale multiloop type reactors. The steam generators (SGs) have been considered as passive safety cooling devices to provide primary loop decay heat removal capacity. There is no additional power supply needed for SGs cooling features. It is specially fit for nonloss of coolant accident applications. The steam released from SGs will be condensed in an accessory heat exchanger, which is located in a tank and submerged in low temperature coolant. To enhance the passive safety function and provide a redundant heat removal path, the secondary side passive cooling system will be necessary for advanced reactors.

In order to improve the security and reliability of reactor, some evolutionary and innovative reactors, such as AP600/1000, WWER640/407, APR+, SBWR, and SMART, employ passive residual heat removal systems [1]. But most of these systems are primary passive cooling systems, except for WWER640/407 and APR+. The passive heat removal system for the WWER640/407 reactor is located at the secondary side of SG. In case of non-LOCAs the decay heat is removed by coolant natural circulation to steam generator boiler water. The steam generated comes into the passive heat removal

system where steam is condensed on the internal surface of the tubes that are cooled on the outside surface by the water stored in the demineralized water tank outside the containment. The water inventory in this tank is sufficient for the long-term heat removal (at least 24 hours) and can be replenished if necessary from an external source [2].

The APR+ is a Generation III+ nuclear power plant being developed in Korea. The passive auxiliary feedwater system (SG secondary side passive residual heat removal system) is one of the advanced safety features being adopted in the APR+. It cools down the secondary side of the steam generator and eventually removes the decay heat from the reactor core by adopting a natural circulation mechanism, that is, condensing steam in the nearly horizontal passive condensation heat exchanger tubes submerged inside the passive condensation cooling tank [3].

The SG secondary side passive residual heat removal system (PRHRS), which removes the residual heat when station blackout occurs, is considered in Chinese advanced PWR. The passive residual heat removal system eliminates a great deal of water in the condensation tank, which is cooled by air natural circulation in the chimney. Only a small quantity of water in the emergency feedwater tank is needed for absorption of residual heat at the initial period of accident.

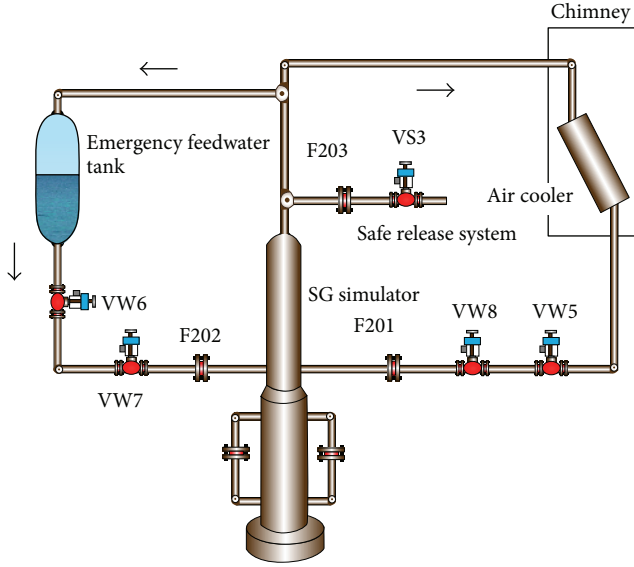


FIGURE 1: Schematic diagram of PRHRS test facility.

In order to assess the ability of PRHRS, experimental research had been done at advanced PWR PRHRS test facility in Nuclear Power Institute of China; in the meantime, the computer code MISAP2.0 has been developed and verified.

2. Test Facility

The test facility has been built according to two-phase natural circulation scaling methodology laws. The geometrical similarity, friction number, density ratio, Froude number, phase change number, and drift-flux number are the important similarity groups. And it is composed of steam-water circulation loop, emergency feedwater loop, air natural circulation loop, and safe release system. The main components include steam generator, air cooler, emergency feedwater tank (EFWT), and chimney. It has a geometrical scaling ratio of 1/390 in volume, and the total height from the top of the height-adjustable chimney to the bottom of SG is about 23 m. The maximal pressure of facility is 8.6 MPa, and the core decay heat is simulated by electric heaters with a capacity of 400 kW (DC). Figure 1 shows its schematic diagram.

The work principle of test facility is as follows. When station blackout or other accidents occur, the isolation valves located at the outlet pipe of emergency tank are opened by a low-low water signal for the SG, so that the emergency water tank provides water to the secondary side of SG driven by gravity and maintains the water level. The water in the SG absorbs the residual heat when the water evaporates. The steam rises and passes through the air cooler where the steam is condensed into water; simultaneously, the heat is transferred into the air through the air natural circulation composed of chimney and atmosphere. Then, the condensed water returns to the SG loop driven by gravity; thereby, a continuous natural circulation flow is established.

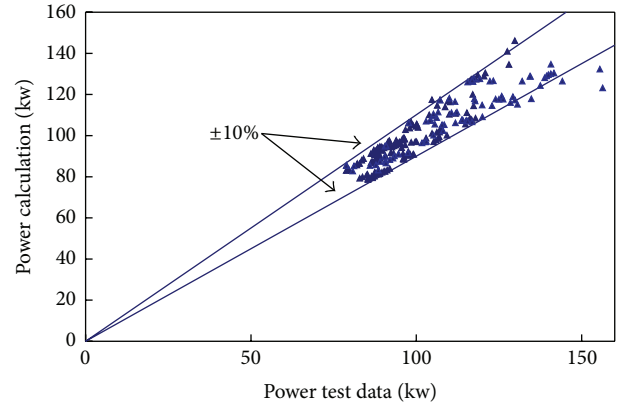


FIGURE 2: Power comparison between test and calculation.

3. Test Matrix and Startup Modes

A total of 280 sets of experimental data at steady state have been obtained and the main influence factors on heat removal capability were identified. The main operation parameters are the height of chimney, the hydraulic resistance, and the initial pressure.

More than 30 transient tests had been performed while the residual heat drops from 8% full power to 2% full power (Figure 2). In addition the influence factors on flow instability were identified.

4. Test Results and Analysis

4.1. Steady Test. The natural circulation is influenced by many parameters, such as the height of chimney, the hydraulic resistance, and the initial pressure. Several tests are implemented to investigate the effect of these parameters on the passive residual heat removal system. In addition a semiempirical model was generated for predicting the natural circulation behavior of Chinese advance pressurized water reactor.

The equation of momentum for passive residual heat removal loop is

$$(\rho_w L_w - \rho_s L_s - \rho_{sg} L_{sg}) g = \frac{k_w w^2}{2\rho_w A_w^2} + \frac{k_s w^2}{2\rho_s A_s^2}, \quad (1)$$

where the subscripts w , s , and sg are water in the down pipe, steam in the rise pipe, and SG respectively.

Equation of momentum for air loop is

$$(\rho_y - \rho_{yi}) g L_y = \frac{k_y w_a^2}{2\rho_y A_y^2}, \quad (2)$$

where the subscripts y and yi are outlet and inlet of chimney, respectively.

The air cooler heat transfer equation is

$$Q = KF\Delta T_m. \quad (3)$$

In steam side of the cooler,

$$Q = W(H_s - H_w). \quad (4)$$

TABLE 1: Effect of the height of chimney.

Number	Height of chimney (m)	Test			Calculation		
		Natural circulation flow rate (kg/h)	Temp. of condensate (°C)	Power (kW)	Natural circulation flow rate (kg/h)	Temp. of condensate (°C)	Power (kW)
1	9.7	204.4	280.2	86.7	210.3	277.09	90.8
2	14.1	226.4	279.6	96.5	236.7	278.66	101.7
3	14.8	230.9	280.9	97.2	235.6	273.87	102.8
4	21.1	238.5	263.1	107.4	249.5	256.16	115.1
5	27.1	249.0	243.7	119.1	259.3	237.96	125.8

The height between air cooler and SG is 14.5 m, the hydraulic resistance is 105, the water in SG is 5.1 m, the pressure is 6.4 MPa, and the temperature at the inlet is 20°C.

TABLE 2: Effect of the hydraulic resistance.

Number	Hydraulic resistance (m)	Test		Calculation	
		Natural circulation flow rate (kg/h)	Power (kW)	Natural circulation flow rate (kg/h)	Power (kW)
1	86	215.6	89.4	227	92.7
2	122	211.0	88.5	221	91.9
3	153	210.1	88.2	220	92.7
4	157	209.4	87.9	219	92.5
5	171	206.7	87.6	217	91.7

The height between air cooler and SG is 14.5 m, the height of chimney is 10.5, the water in SG is 5.1 m, the pressure is 6.4 MPa, and the temperature at the inlet is 20°C.

In air side of the cooler,

$$Q = W_a (H_y - H_{yi}), \quad (5)$$

where K is heat transfer coefficient, F is heat transfer area, ΔT_m is mean temperature difference, and W_a is the air flow rate.

Coupling with (1)–(5), a semiempirical correlation has been built up for total PRHR system heat transfer estimation based on the test results. In this case, when system pressure, water level in SG, friction coefficient, and the height between SG and air cooler are given, the ability of heat removal can be calculated. Consider

$$Q = 268 \times \frac{(0.98 - Lth/30)^{-0.05} \times (0.8LnH + 1.2)}{(7.06 - 1.23LnP) e^{(0.05/100)K} \times t_{in}^{0.2}}. \quad (6)$$

Sensitivity studies on different structure parameters have been made. The results will be described in detail as follows.

4.1.1. Effect of the Height of Chimney. The effect of the height of chimney in the passive residual heat removal system has been identified at the initial height of chimney of 9.7 m and 27.1 m. In this group of sensitive studies, the hydraulic resistance hardly keeps the same value under different condition, which is maintained at less than 10%. And the temperature of air at the inlet of chimney and pressure are unchanged values with only the height being allowed to change to find the effect.

Table 1 shows the experimental data and calculation of the natural circulation flow rate, power, and temperature of condensate, respectively. As the height of chimney increases, the natural circulation flow rate of air loop and power of air cooler rise. Then, the temperature of condensate decreases.

When the height between air cooler and SG and hydraulic resistance is constant, the reduced density of condensate causes the increase of natural circulation flow rate. In addition the calculation shows good agreement with experimental data.

4.1.2. Effect of the Hydraulic Resistance. The effects of the hydraulic resistance (frictional resistance and local resistance) in the passive residual heat removal system are performed in this study (Table 2). Other parameters are kept at a constant value. The hydraulic resistance is varied from 86 to 171. We can see that the resistance increases more than 100%, but the natural circulation flow rate and power decrease rarely. Therefore, the hydraulic resistance has little influence on the passive residual heat removal system.

4.1.3. Effect of the Initial Pressure on the Passive Residual Heat Removal System. The initial pressure in the passive residual heat removal system changes from 3.53 MPa to 7.30 MPa, and other parameters are fixed except for the hydraulic resistance with a 10 percent deviation. As the pressure ascends, the increase of power and natural circulation flow rate is 22.3% and 25%, respectively (Table 3).

4.2. Transient Test. When the station blackout accident happens in the Chinese advance pressurized water reactor, it adopts the passive residual heat removal system to mitigate consequences of accidents. The passive residual heat removal system startup modes include warm and cold patterns when the emergency feedwater is on or off, respectively. If there is a tiny flow rate to keep a little natural circulation in both steam-water circulation loop and air natural circulation loop

TABLE 3: Effect of the initial pressure.

Number	Pressure (MPa)	Test		Calculation	
		Natural circulation flow rate (kg/h)	Power (kW)	Natural circulation flow rate (kg/h)	Power (kW)
1	3.53	151.0	76.1	153.2	74.7
2	4.51	160.2	80.8	161.6	80.2
3	6.82	170.3	88.0	163.0	86.2
4	7.80	188.3	93.6	176.7	89.5

The height between air cooler and SG is 14.5 m, the height of chimney is 12.8, the water in SG is 5.1 m, the hydraulic resistance is 105, and the temperature at the inlet is 33°C.

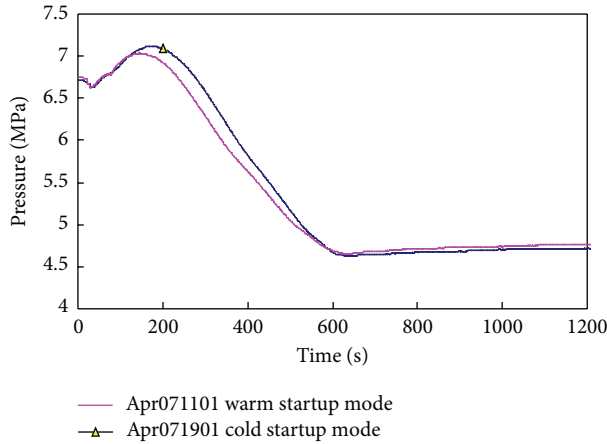


FIGURE 3: The pressure of cold and warm startup mode.

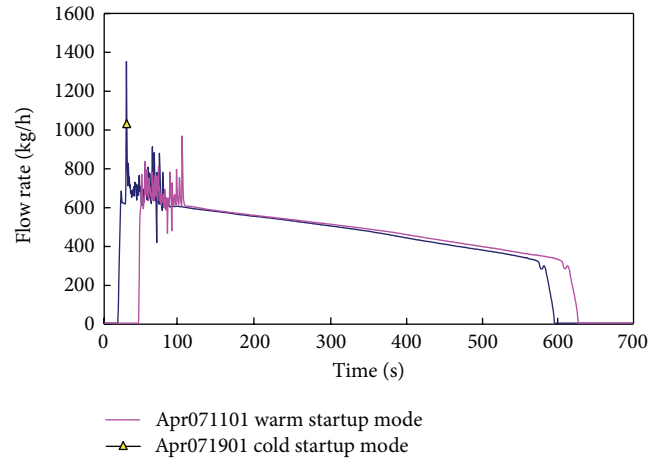


FIGURE 5: The feedwater flow rate.

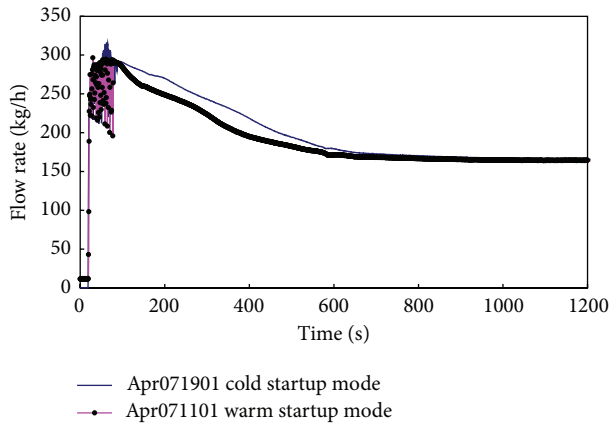


FIGURE 4: The natural circulation flow rate.

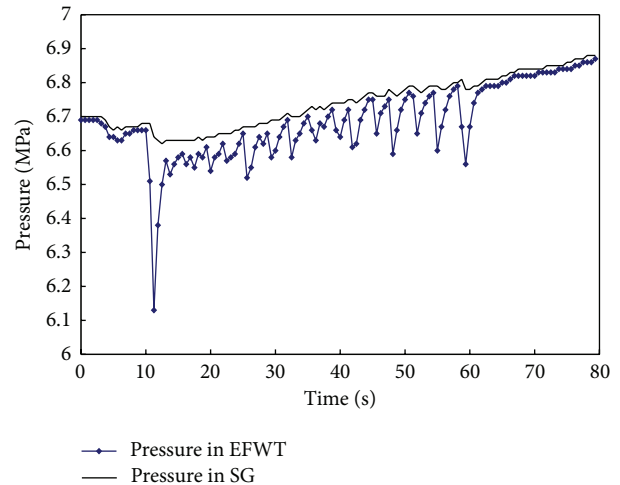


FIGURE 6: The pressure fluctuation when water hammer occurs.

before the startup of transient test, this type of startup mode is defined as warm startup. On the other hand, if the initial condition is cold, or there is no flow in both steam-water circulation loop and air natural circulation loop, this type of startup mode is defined as cold startup.

The typical results of cold and warm startup tests with emergency feedwater are shown in Figures 3–6. The pressure increases before the air natural circulation is established when the residual heat is larger than that absorbed by cold water in air cooler and EFWT. But the pressure begins to drop not only because of the residual heat decay but also

because the air flow rate reaches its maximum. As shown in Figure 3, there is no remarkable difference between cold and warm startup. Figure 4 shows the natural circulation. As the isolation valve is open, the natural circulation is established between SG and air cooler. The flow rate rises to 300 kg/h. The flow instability happens at the beginning of natural circulation, which is caused by the water hammer that occurs in emergency feedwater tank. The water hammer also results in flow instability of injection from emergency feedwater tank

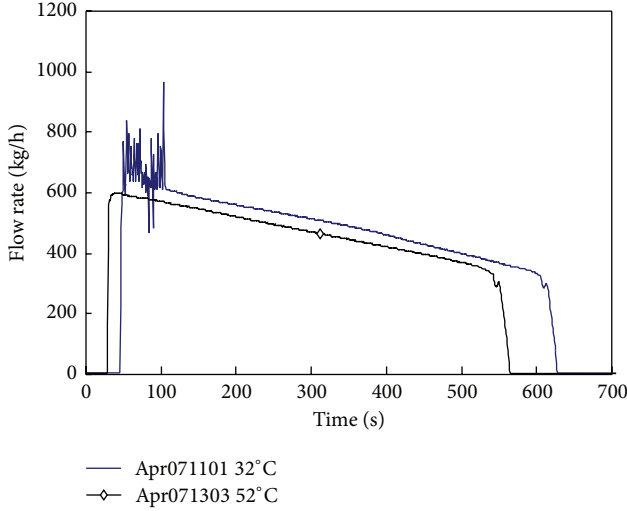


FIGURE 7: Water hammer influenced by feedwater temperature.

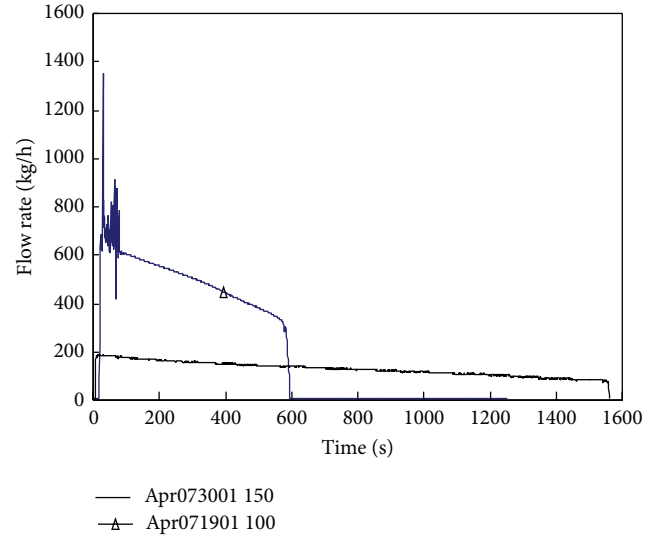


FIGURE 8: Water hammer influenced by resistance of feedwater loop.

as shown in Figure 5. The water hammer occurs in emergency feedwater tank when a great deal of steam, which is rushing into emergency feedwater tank through the pressure balance pipe after the feedwater valve is opened, condenses quickly. The pressure fluctuates in the emergency feedwater tank when the water hammer happens as shown in Figure 6. Some tests have been performed to avoid water hammer's appearance.

4.2.1. Effect of Temperature of Feedwater. The effect of temperature of feedwater in the passive residual heat removal system has been identified at the initial temperatures of 32°C and 52°C and the other parameters are kept at a constant value. The results are shown in Figure 7. When the temperature of feedwater in the emergency feedwater tank is 52°C, the water hammer does not happen because the direct contact condensation is related to the temperature of fluid.

4.2.2. Effect of Resistance of Feedwater Loop. In this group of case studies, the resistance of feedwater loop is changed by +50% of the reference case, and the other parameters are the same. The results are shown in Figure 8. As the resistance of feedwater loop increases, the feedwater flow rate and steam flow rate decrease accordingly. As a result there is not flow instability.

5. Code Development and Verification

MISAP2.0 code is a typical code that is used to analyze steady and transient performance of the secondary passive residual heat removal system.

5.1. Mathematical Model. A basic assumption is that one-dimensional approach is used.

5.1.1. Single-Phase Conservative Equations. Equation of continuity is

$$\frac{\partial \rho}{\partial \tau} + \frac{1}{A} \frac{dW}{dZ} = 0, \quad (7)$$

where W is flow rate and ρ is density.

Equation of momentum is

$$\frac{\partial W}{\partial \tau} = -A \frac{\partial P}{\partial Z} - \frac{\partial}{\partial Z} \left(\frac{W^2}{\rho A} \right) - \rho g A - U_h f \frac{W^2}{2\rho A^2}, \quad (8)$$

where A is the cross-sectional area of the flow channel; P is pressure; U_h is wetted perimeter; f is friction coefficient; g is the gravitational acceleration.

Equation of energy is

$$\frac{\partial}{\partial \tau} \left[\rho \left(u + \frac{V^2}{2} \right) \right] + \frac{\partial}{\partial Z} \left[\rho \left(u + \frac{V^2}{2} \right) V \right] \quad (9)$$

$$= \frac{qU_k}{A} + \frac{1}{A} \int_A q_V dA - \frac{\partial}{\partial Z} (VP) - \rho g V,$$

where h is enthalpy; V is velocity; q_V is heat generation rate of the fluid; U_k is heated perimeter. The gravitational work and the work related to the kinetic energy variation can be neglected and the heat generation of the fluid is ignored; the equation can be simplified as follows:

$$\rho \frac{\partial h}{\partial \tau} + \frac{W}{A} \frac{\partial h}{\partial Z} = \frac{qU_h}{A} + \frac{\partial P}{\partial t}. \quad (10)$$

5.1.2. Two-Phase Mixture Conservative Equations. Equation of continuity is

$$\frac{\partial}{\partial t} [\alpha \rho_g + (1 - \alpha) \rho_f] + \frac{1}{A} \frac{\partial W}{\partial Z} = 0, \quad (11)$$

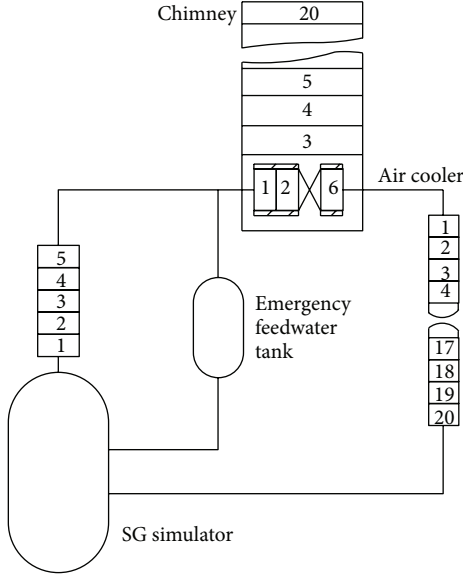


FIGURE 9: MASAP nodalization diagram of the test facility.

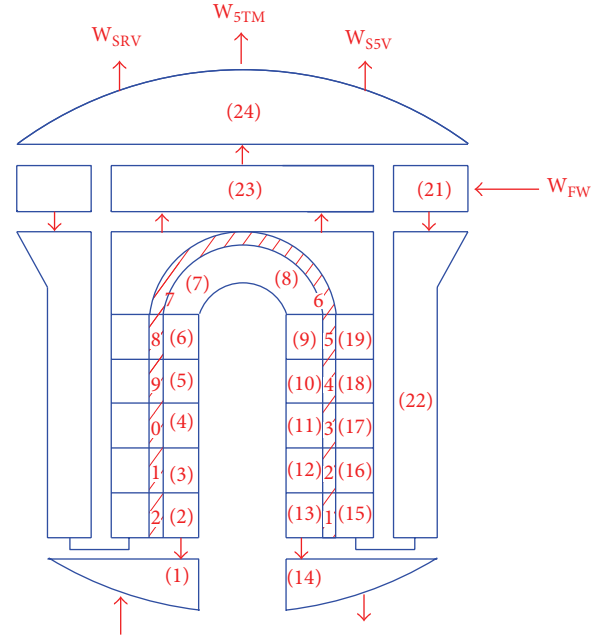


FIGURE 10: MASAP nodalization diagram of SG.

where α is void fraction; subscripts g and f stand for steam and saturated liquid, respectively.

Equation of momentum is

$$\frac{\partial}{\partial \tau} (\rho V) + \frac{\partial}{\partial Z} (\rho V^2) = -\frac{\partial P}{\partial Z} - \frac{1}{A} \int_U \tau_f dU - \rho g. \quad (12)$$

Equation of energy is

$$\frac{\partial}{\partial t} [(1 - \alpha) \rho_f h_f + \alpha \rho_g h_g] + \frac{1}{A} \frac{\partial}{\partial Z} [Wh] = \frac{qU_h}{A} + \frac{\partial P}{\partial t}. \quad (13)$$

5.1.3. *Emergency Feedwater Tank.* Consider

$$W_{\text{tank}} = \sqrt{\frac{2g\Delta H}{\xi}} \rho A_{\text{tank}}. \quad (14)$$

5.1.4. *Air Loop.* Momentum equation is

$$\begin{aligned} \frac{\partial W_a}{\partial \tau} \int_0^{L_y} \frac{1}{A} dz = & - \int_0^{L_y} \frac{\partial P}{\partial Z} dz - \int_0^{L_y} \frac{1}{A} \cdot \frac{\partial}{\partial z} \left(\frac{W_a^2}{\rho A} \right) dz \\ & - \int_0^{L_y} \rho g dz - W_a^2 \int_0^{L_y} \frac{U_h}{A} f \frac{1}{2\rho A^2} dz, \end{aligned} \quad (15)$$

where L_y is the chimney height.

5.2. *Numerical Model.* In view of the fact that two loops closely couple with each other due to energy and momentum interactions, the two loops are solved together. Figures 9 and 10 show MASIP2.0 nodalization diagram of test facility and SG. After the discretization of the spatial derivative terms in

the equations, the following ordinary differential equations are obtained:

$$\begin{aligned} \frac{d\vec{y}}{dt} &= \vec{f}(t, \vec{y}, \vec{y}'), \\ \vec{y}(t_0) &= \vec{y}_0. \end{aligned} \quad (16)$$

Therefore, the whole system dynamic simulation can be solved as an initial value problem. For the stiff system of differential equations, Gear's algorithm is used traditionally.

5.3. *Steady State Calculation.* During the steady state calculation, several parameters, such as natural circulation flow rate, flow rate of air, temperature of condensate, and air at outlet of chimney, are calculated. And the calculations of MASIP2.0 are compared with the experimental data shown in Table 4. It shows that the error between calculation and experimental data is less than 10%.

5.4. *Transient State Calculation.* The transient calculation results of cold startup model test are compared with experimental data in Figures 11 and 12. Figure 11 shows the pressure comparison between calculation and test. The pressure increases before the air natural circulation is established when the residual heat is larger than that absorbed by cold water in air cooler and EFWT. MASIP2.0 code predicts the pressure well. However, the quantitative description is poor in the initial period of the transient. The reason is that there is no direct contact condensation model in the code. Then, the calculated flow rate of feedwater is less than experimental data, as shown in Figure 12. As a result the calculation of pressure is higher than that in the tests. As for the absence of direct contact condensation model, the water hammer is not observed.

TABLE 4: Comparison between the calculation of MISAP2.0 and experimental data.

Number	Test				Calculation of MISAP2.0			
	Natural circulation flow rate (kg/h)	Temp. of condensate (°C)	Flow rate of air (kg/s)	Temp. of air at outlet (°C)	Natural circulation flow rate (kg/h)	Temp. of condensate (°C)	Flow rate of air (kg/s)	Temp. of air at outlet (°C)
1	184.0	218.5	0.581	184.3	194.6	218.3	0.600	184.1
2	165.8	194.9	0.582	185.5	183.4	216.9	0.595	177.6
3	198.8	255.2	0.579	181.2	219.9	249.6	0.609	202.1
4	164.6	229.3	0.515	193.0	180.6	246.3	0.550	188.6

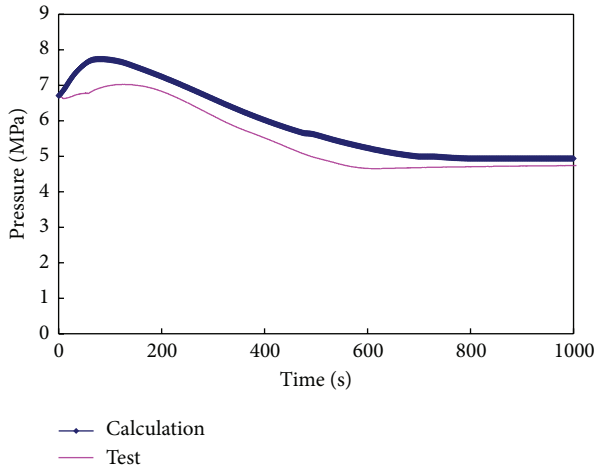


FIGURE 11: The pressure comparison between calculation and test.

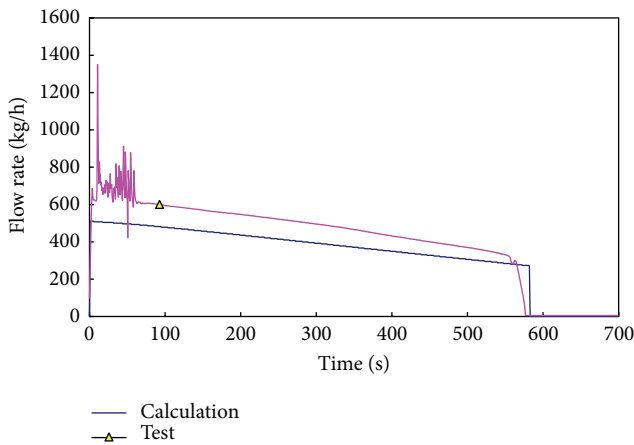


FIGURE 12: The flow rate comparison between calculation and test.

6. Conclusion

The passive residual heat removal system (PRHRS) characteristics of Chinese advance pressurized water reactor (CAPWR) have been experimentally investigated. Based on the investigations, the following conclusions are drawn.

- (1) A total of 280 sets of tests at steady state have been implemented to investigate the effect of some parameters on the passive residual heat removal system.

The result shows that the height of chimney has great influence on natural circulation flow rate. And the effect of the initial pressure and hydraulic resistance is small or negligible.

- (2) Based on the experiments, semiempirical model for analyzing passive residual heat removal system is established, and the calculation shows good agreement with experimental data. It can be applied to system arrangement design for PRHRS of Chinese advanced PWR.
- (3) In case of station blackout accident, the transient characteristics of passive residual heat removal system were studied. The natural circulation and injection of feedwater are very useful for removal of decay heat.
- (4) The increase of feedwater's initial temperature and resistance of feedwater loop is useful to avoid the water hammer.
- (5) A code MISAP2.0 has been developed, and the transient tests are used to verify the prediction of MISAP2.0. The calculated parameter variation trend is reasonable. However, the flow fluctuation and water hammer cannot be simulated by MISAP2.0. Now the direct contact condensation is under development for next version of MISAP.

Nomenclature

- A : Flow area (m^2)
- f : Friction factor
- g : Gravity acceleration (m/s^2)
- h : Specific enthalpy (J/kg)
- K : Loss coefficient
- H : Emergency feedwater tank water lever (m)
- P : Pressure (Pa)
- q : Heat flux (W/m^2)
- t : Time (s)
- U : Heated perimeter (m)
- U_e : Wetted perimeter (m)
- W : Mass flow rate (kg/s)
- z : Special coordinate (m)
- α : Void fraction
- ρ : Density (kg/m^3).

Conflict of Interests

The authors declare that there is no conflict of interests regarding the publication of this paper.

References

- [1] "Passive safety systems and natural circulation in water cooled nuclear power plants," IAEA-TECDOC-1624, IAEA, Vienna, Austria, 2009.
- [2] "Status of advanced light water reactor designs 2004," IAEA-TECDOC-1391, IAEA, Vienna, Austria, 2004.
- [3] S. Kim, B. Byoung-Uhn, C. Yun-Je, P. Yu-Sun, K. Kyoung-Ho, and Y. Byong-Jo, "An experimental study on the validation of cooling capability for the passive auxiliary feedwater system (PAFS) condensation heat exchanger," *Nuclear Engineering and Design*, vol. 260, pp. 54–63, 2013.



Hindawi

Submit your manuscripts at
<http://www.hindawi.com>

